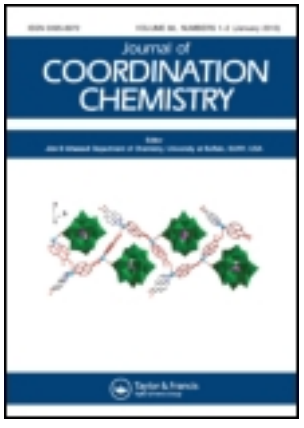

Journal of Coordination Chemistry
Publication details, including instructions for authors and subscription information:
http://www.tandfonline.com/loi/gcoo20

Iron complexes with gallic acid: a computational study on coordination compounds of interest for the preservation of cultural heritage

Sara Zaccaron [a], Renzo Ganzerla [a] & Marco Bortoluzzi [a]
[a] Dipartimento di Scienze Molecolari e Nanosistemi, Università Ca' Foscari Venezia, Venezia, Italy
Accepted author version posted online: 26 Mar 2013.Published online: 02 May 2013.

To cite this article: Sara Zaccaron, Renzo Ganzerla & Marco Bortoluzzi (2013) Iron complexes with gallic acid: a computational study on coordination compounds of interest for the preservation of cultural heritage, Journal of Coordination Chemistry, 66:10, 1709-1719, DOI: 10.1080/00958972.2013.790019

To link to this article: http://dx.doi.org/10.1080/00958972.2013.790019

Journal of Coordination Chemistry, 2013
Vol. 66, No. 10, 1709–1719, http://dx.doi.org/10.1080/00958972.2013.790019

Iron complexes with gallic acid: a computational study on coordination compounds of interest for the preservation of cultural heritage

SARA ZACCARON*, RENZO GANZERLA and MARCO BORTOLUZZI

Dipartimento di Scienze Molecolari e Nanosistemi, Università Ca' Foscari Venezia, Venezia, Italy

(*Received 17 December 2012; in final form 27 February 2013*)

The electronic structures of iron coordination compounds $[FeL_4H_{12}]^-$, $[FeL_4H_{12}]^{2-}$, $[Fe_3L_8H_{22}]^-$, and $[Fe_3L_8H_{22}]^{2-}$ (H_4L = gallic acid, 3,4,5-trihydroxybenzoic acid) have been studied by density functional theory calculations, together with the 1-D periodic complex $[Fe_3L_6H_{15}]_\infty$. Data regarding the ground-state spin multiplicities of these models for iron gall inks, the charge and spin distributions, the oxidation states of the metal centers, and the oxidizing potentials of the complexes have been computed. The absorption properties of these compounds have been related to the electronic structure of the coordinated ligands.

Keywords: Iron; Gallic acid; Gall inks; Cultural heritage; DFT

1. Introduction

Iron gall complexes are the main components of iron gall inks, which have been the most used writing materials since the beginning of the eleventh century [1]. The ancient procedure for preparation of these inks generally requires three main ingredients: tannins extracted from plants (usually from gall nuts), vitriol (an historic term commonly referred to iron(II) sulfate heptahydrate), and a binder such as arabic gum. Iron gall complexes can be currently synthesized by reacting an iron(II) salt, for example iron sulfate, with gallic acid (3,4,5-trihydroxybenzoic acid) under aerobic conditions in acidulated water. However, iron gall derivatives can be obtained also starting from iron(III) salts, as an example hydrated $FeCl_3$.

Molecular structures of most of the iron coordination compounds present in iron gall inks are still not completely ascertained. Single-crystal X-ray diffraction measurements have been carried out by Wunderlich and co-workers on the product formed by reaction of iron(III) chloride and gallic acid [2], which have formula $[Fe(H_3O)(H_2O)(L)]_n$ (H_4L = gallic acid). To the best of our knowledge, this compound is the only structurally characterized iron gall ink. This species is a 3-D periodic polymer (trigonal space group, $a = 8.664$ Å, $b = 8.664$ Å, $c = 10.861$ Å, $\alpha = 90°$, $\beta = 90°$, $\gamma = 120°$, cell volume = 706.05 Å^3, symmetry

*Corresponding author. Email: sara.zaccaron@unive.it

group $P3_121$) where several iron ions are bridged by the conjugate base of gallic acid. The iron centers have slightly distorted octahedral geometry with six Fe–O bonds. Two oxygens mutually in *cis* position belong to two separate carboxylic moieties and the corresponding Fe–O bond lengths are 2.006 Å. Two L are mutually *cis* and coordinate iron, each with two phenate-type oxygens. The corresponding Fe–O bonds are 2.000 (oxygen in positions 3 and 5) and 2.028 Å (oxygen in position 4). Each carboxylate is a bridging ligand between two iron centers, whereas the three phenate-type oxygens of every ligand chelate two metal ions. The oxygen atom in *para* position with respect to carboxylate acts as bridging atom. The 3-D structure of $[Fe(H_3O)(H_2O)(L)]_n$, the inner coordination sphere of the iron centers and the coordination of the conjugate base of gallic acid to the metal ions are reported in figures 1 and 2 for clarity.

The deep blue color of iron gall species is attributable to a strong electronic delocalization among the metal ions, but the lack of detailed studies in the current literature make the real oxidation and spin states of the iron centers not unambiguously ascertained. Besides interest towards light absorption properties of these materials, important historical objects in libraries and archives show noticeable degradation caused by the destructive effects of metallo-gallate inks interacting with cellulose and sizing. Comparable degradation effects are also known for other substrates of interest for cultural heritage, for example wool fibers. The chemical phenomenon of corrosion caused by iron gall inks has been intensively studied for many years, and acid hydrolysis and after-effects of Fenton reactions have been blamed [3]. Unfortunately, the incomplete information in the literature about electronic features of iron gall inks makes some degradation pathways unclear.

A deeper knowledge about the electronic configuration of these inks is therefore of paramount interest for the development of methodologies useful for preservation and restoration of cultural heritage. For these reasons, as a continuation of our recent computational studies on coordination chemistry of group eight elements [4], in the present article we report a computational density functional theory (DFT) study on the electronic structure of mono- and tri-nuclear coordination compounds, which have been used as simplified models for iron gall inks.

2. Computational details

Model compounds $[FeL_4H_{12}]^{n-}$ and $[Fe_3L_8H_{22}]^{n-}$ ($n = 1, 2$) have been built on the basis of the deposited X-ray data regarding the isolated product of the reaction between iron(III) chloride and gallic acid [2]. The internal coordinates concerning the conjugate base of gallic acid (L) and its interactions with iron centers have not been changed with respect to the experimental values. Hydrogens have been added to carbons of L in position two and six and their coordinates have been optimized using the MMFF94 force field, keeping all the other atoms frozen [5]. Further, hydrogens have been added on phenate and carboxylate oxygens to achieve the desired charge and their positions have been optimized using MMFF94. Cartesian coordinates of the structures are collected in the Supplementary Materials file. Also, the 1D periodic complex $[Fe_3L_6H_{15}]_\infty$ has been built on the basis of reported experimental data [2]. Periodicity along the translation vector c (10.861 Å) has been maintained with respect to the original structure, together with all the internal coordinates. Hydrogens have been added on the phenyl rings in positions two and six and on oxygens to obtain a neutral primitive cell. A mesh of 62 points has been used for the sampling of the reciprocal space [6].

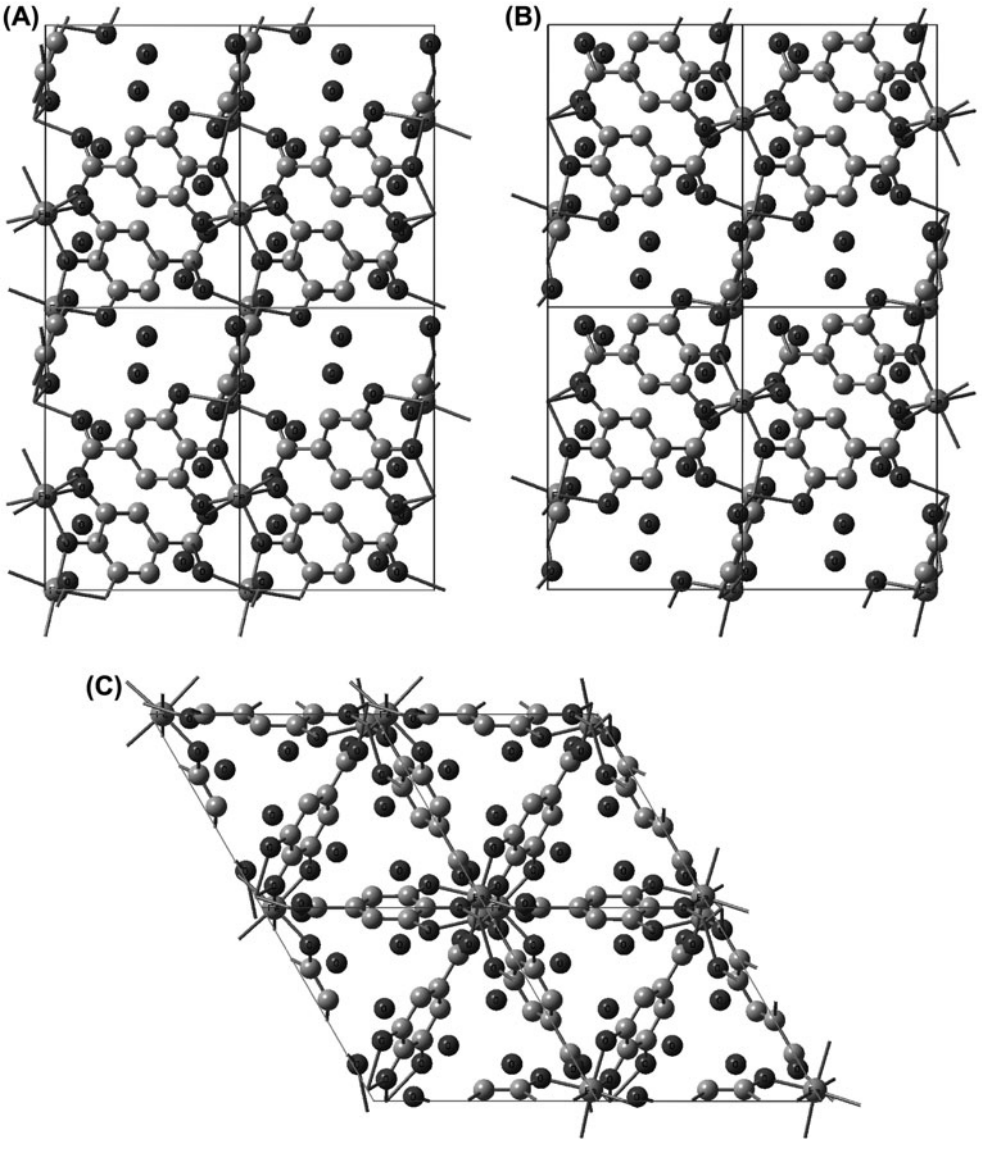

Figure 1. Structure of $[Fe(H_3O)(H_2O)(L)]_n$. (A) View along a vector. (B) View along b vector. (C) View along c vector. Data are from [2].

DFT calculations have been carried out without symmetry constraints using a pure DFT Generalized Gradient Approximation (GGA) functional (PBEPBE [7]) and two hybrid DFT functionals (B3PW91 [8], M06 [9]) in combination with split-valence double- and triple-ζ quality basis sets and small-core pseudopotentials for the irons. In particular, double-ζ quality calculations have been performed using the D95 V [10] basis set for carbon, oxygen, and hydrogen and the ECP-based SDD basis set for iron [11]. A further refining has been carried out for selected cases using the polarized 6-311G(d,p) basis set on C, O, and H [12] and the polarized ECP-based LANL2TZ(f) basis set on Fe [13].

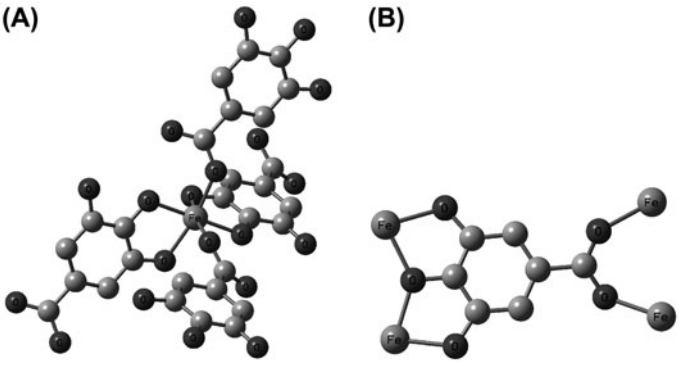

Figure 2. (A) Octahedral coordination sphere around each iron center in $[Fe(H_3O)(H_2O)(L)]_n$. (B) Coordination of L to the iron centers in $[Fe(H_3O)(H_2O)(L)]_n$. Data are from [2].

Implicit solvation has been added for non-periodic models by applying the C-PCM model for water using Universal Force Field atomic radii [14]. The same computational approaches have been applied for the optimization of $[Fe(H_2O)_6]^{n+}$ ($n=2$, sextet state; $n=3$, quintet state) and $[Fe(EDTA)]^{n-}$ ($n=1$, sextet state; $n=2$, quintet state; H_4EDTA = ethylenediaminetetraacetic acid). Cartesian coordinates of the optimized complexes are collected in the Supplementary material.

The simulations of the UV–VIS transitions of the radical species $[L]^{3-}$, $[H_2L]^{-}$, and $[H_3L]$ (doublet state; hydrogens on the phenate oxygens) have been carried out, after geometry optimization, on the basis of the TD-SCF approach [15]. The DFT methods here applied have been verified by comparing the simulated (harmonic approximation) and experimental IR spectra of gallic acid [15]. Spectra are reported in the Supplementary file.

In all calculations the unrestricted approach has been used and the absence of meaningful spin contamination has been verified through comparison of the computed $<S^2>$ values with the theoretical ones [15]. Population analyses have been performed on the basis of the Mulliken, Natural and Hirshfeld distributions [16].

All calculations based on DFT have been carried out with Gaussian 09 [17]. Preliminary MMFF94 optimizations of the positions of the hydrogens have been performed with Spartan 08 [18].

3. Results and discussion

The structures of $[FeL_4H_{12}]^{n-}$, $[Fe_3L_8H_{22}]^{n-}$ ($n=1$, 2), and $[Fe_3L_6H_{15}]_\infty$ (H_4L = gallic acid) are reported in figures 3–5. For all these species electron density is localized on the non-metal atoms and on the C–H, C–C, C–O, and Fe–O bonds but no meaningful direct covalent interaction is present among the metal centers. Calculations have been carried out with several DFT functionals in order to ascertain the ground-state multiplicity of $[FeL_4H_{12}]^{n-}$ and $[Fe_3L_8H_{22}]^{n-}$ ($n=1$, 2). All the computational models used (PBEPBE, B3PW91, and M06 DFT functionals) have led to comparable results and in all the cases the highest multiplicity corresponds to the most stable ground-state electronic structure. In particular, the energy difference between high-spin (sextet state) and low-spin (doublet state) configurations for $[FeL_4H_{12}]^{-}$ is around 60 kcal mol^{-1}. The high-spin state (quintet) of $[FeL_4H_{12}]^{2-}$

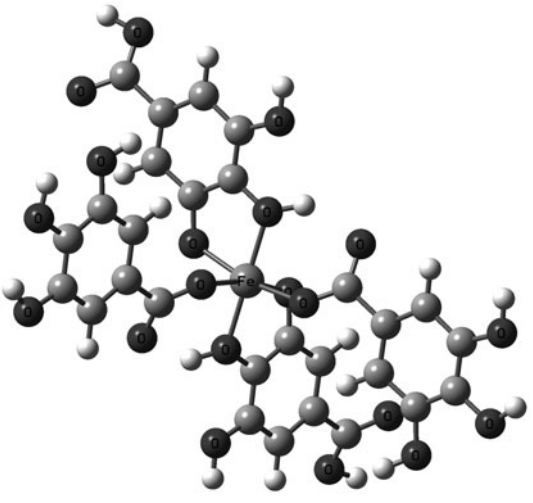

Figure 3. Structures of models $[FeL_4H_{12}]^{n-}$ ($n = 1, 2$).

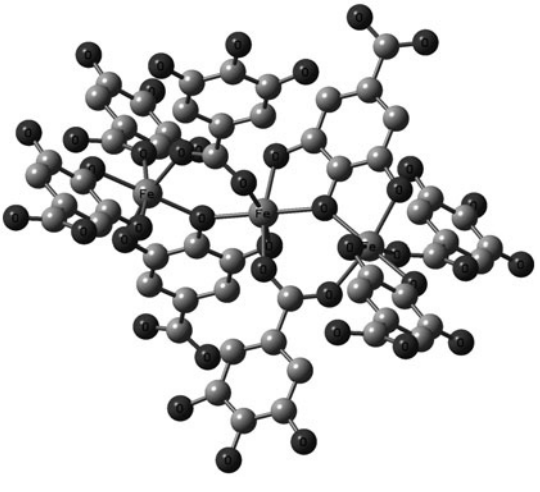

Figure 4. Structures of models $[Fe_3L_8H_{22}]^{n-}$ ($n = 1, 2$). Hydrogens have been omitted for graphical clarity.

is more stable by about 50 kcal mol^{-1} with respect to the singlet configuration. For $[Fe_3L_8H_{22}]^{-}$and $[Fe_3L_8H_{22}]^{2-}$ the pairing of two electrons with respect to the highest multiplicities (15 and 14 unpaired electrons, respectively) causes a strong energy increase, more than 30 kcal mol^{-1} in the first case and about 40 kcal mol^{-1} for the second complex. Additional electron pairings cause a further increase of the total energy for both the models. The greatest stability of the systems having the maximum number of unpaired electrons is confirmed by DFT PBEPBE calculations carried out on the linear periodic model $[Fe_3L_6H_{15}]_\infty$ extrapolated from the original structure. Also in this case, the most stable electronic configuration corresponds to the maximum multiplicity, i.e. 15 unpaired electrons in the primitive cell. The results for spin multiplicity obtained for $[Fe_3L_8H_{22}]^{-}$

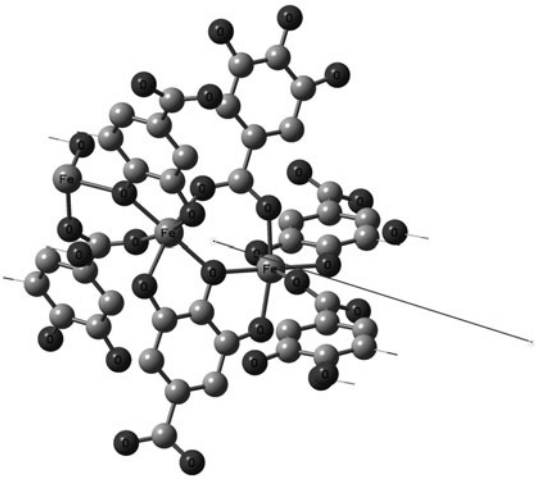

Figure 5. Structure of the primitive cell of $[Fe_3L_6H_{15}]_\infty$ and translation vector. Hydrogens have been omitted for graphical clarity.

and $[Fe_3L_6H_{15}]_\infty$ nicely agree with plane-waves GGA DFT calculations recently carried out on the 3D $[(Fe_3L_3)^{3-}]_\infty$, for which an integral value for spin density over the primitive cell of 7.50 hbar has been computed [19].

Tables 1 and 2 collect the spin densities on the atoms of $[FeL_4H_{12}]^{n-}$ and $[Fe_3L_8H_{22}]^{n-}$ ($n = 1, 2$), taken with their most stable electronic configuration (i.e. highest multiplicity). Spin density is localized on the iron centers and, to a lesser extent, on the phenate and carboxylate oxygens bonded to iron (see for example figure 6), while it is meaningfully lower on the other oxygens and on carbon of the aromatic rings and of the carboxylates. Finally, spin density is virtually zero on hydrogens.

The expected electronic structures for $[FeL_4H_{12}]^-$ and $[Fe_3L_8H_{22}]^-$ are formally iron (III) complexes stabilized by diamagnetic conjugate bases of gallic acid. However, data reported in tables 1 and 2 do not support such an idea. In fact, in all the cases spin densities are meaningfully closer to the values expected for high-spin iron(II) and detailed population analyses, based on both the Mulliken and the Natural approaches, are in agreement with a d^6 configuration of the iron centers, with five up electrons and one down electron.

Table 1. Atomic spin densities (M06/C-PCM calculations, a.u., average values) for $[FeL_4H_{12}]^{n-}$ ($n = 1$, sextet; $n = 2$, quintet).

	$[FeL_4H_{12}]^-$		$[FeL_4H_{12}]^{2-}$	
Atom	Mulliken	Hirshfeld[a]	Mulliken	Hirshfeld[a]
Fe[b]	4.1756	4.1166	3.7710	3.6254
O (Fe–O carboxylate)	0.0993	0.1048	0.0132	0.0408
O (Fe–O phenate)	0.1279	0.1319	0.0303	0.0523
O (not coordinated)	0.0019	0.0017	0.0012	0.0013
C (carboxylate)	−0.0005	0.0033	0.0058	0.0051
C (phenate)	0.0038	0.0046	0.0017	0.0019
H(CH)	−0.0004	–	0.0000	–
H(OH)	0.0002	–	0.0001	–

[a]Hydrogen atoms summed into heavy atoms. [b]Natural atomic spin density on Fe for $[FeL_4H_{12}]^- = 3.9860$ a.u.; for $[FeL_4H_{12}]^{2-} = 3.6061$ a.u.

Table 2. Atomic spin densities (M06/C-PCM calculations, a.u., average values) for $[Fe_3L_8H_{22}]^-$ (15 unpaired electrons) and $[Fe_3L_8H_{22}]^{2-}$ (14 unpaired electrons).

	$[Fe_3L_8H_{22}]^-$		$[Fe_3L_8H_{22}]^{2-}$	
Atom	Mulliken	Hirshfeld[(a)]	Mulliken	Hirshfeld[(a)]
Fe[(b)]	4.1832	4.1393	4.1001	4.0312
O (Fe–O carboxylate)	0.0860	0.0940	0.0666	0.0781
O (Fe-O phenate)	0.1628	0.1615	0.1303	0.1293
O (not coordinated)	0.0021	0.0024	0.0005	0.0000
C (carboxylate)	0.0056	0.0080	−0.0179	−0.0019
C (phenate)	0.0047	0.0058	0.0025	0.0031
H(CH)	−0.0002	–	0.0003	–
H(OH)	0.0001	–	0.0001	–

[(a)]Hydrogen atoms summed into heavy atoms. [(b)]Average natural atomic spin density on Fe for $[Fe_3L_8H_{22}]^-$ = 4.0017 a.u.; for $[Fe_3L_8H_{22}]^{2-}$ = 3.9206 a.u.

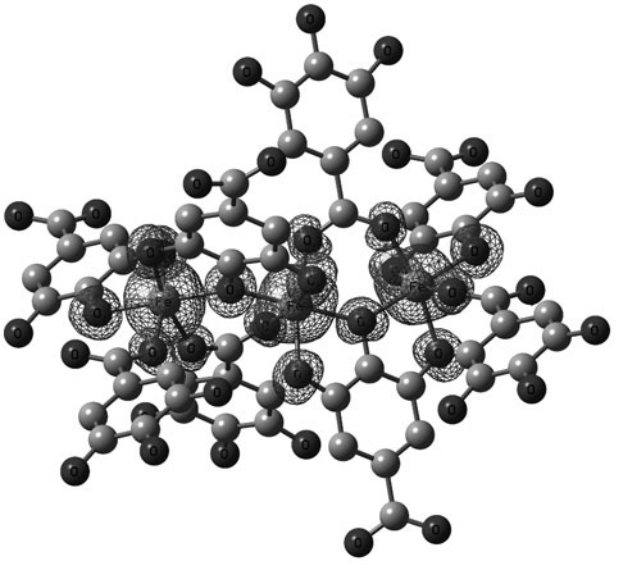

Figure 6. Plot of spin density for $[Fe_3L_8H_{22}]^-$ (15 unpaired electrons, M06/C-PCM). Hydrogens have been omitted for graphical clarity.

The residual spin density, localized on the coordinated oxygens of the ligands, phenate-type in particular, is probably due to the fact that gallic acid molecules in these compounds behave as radical species, because a formal ligand-to-metal reduction has occurred [20]. Comparable results have been obtained from PBEPBE calculations on the 1D coordination polymer $[Fe_3L_6H_{15}]_\infty$, where the average spin density on the iron centers of the primitive cell is about 4 a.u. (Mulliken: 4.108 a.u.; Hirshfeld: 4.080 a.u.), and the residual spin densities are mainly on the coordinated phenate (Mulliken: 0.1481 a.u.; Hirshfeld: 0.1787 a.u.) and carboxylate (Mulliken: 0.1083 a.u.; Hirshfeld: 0.1283 a.u.) oxygens.

The same qualitative picture about gallic acid – iron systems was obtained during our previous studies from plane-waves calculations on the 3D model $[(Fe_3L_3)^{3-}]_\infty$. Also for that system charge and spin distributions suggested the presence of high-spin iron(II)

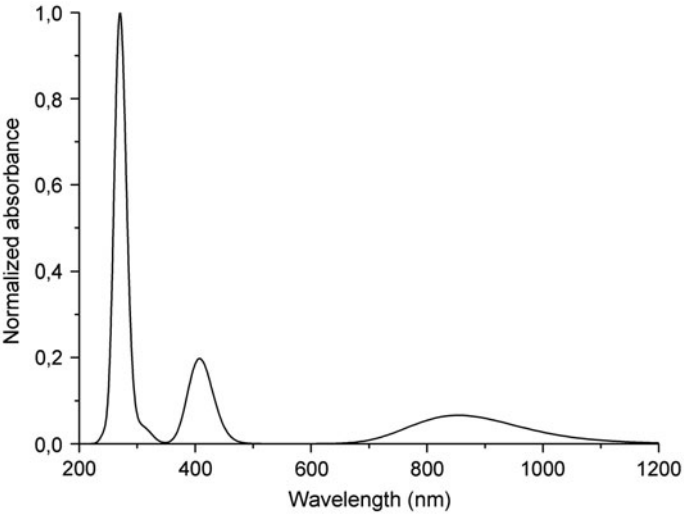

Figure 7. Simulated UV–VIS spectrum of $[L]^{3-}$ (FWHM = 3000 cm^{-1}).

bridged by radical ligands $[L]^{3-}$, formally in doublet state. The similarity of the simulated absorption spectrum with the experimental ones supported the relative accuracy of that model [19]. Therefore, the intense blue color of iron gall inks could be attributed to the pseudo-radical electronic structure of the conjugate bases of gallic acid in iron gall inks. Effectively, simulated UV–VIS spectra of radical species such as $[L]^{3-}$, $[H_2L]^{-}$, and $[H_3L]$ confirm such hypothesis, showing absorption bands centered at the end of the red region or at the beginning of the NIR region. As an example, the simulated UV–VIS spectrum of $[L]^{3-}$ depicted in figure 7 predicts a low-energy band having wavelength comparable with those commonly reported for iron gall inks [1, 2] (see also figures S1 and S2 for examples of experimental spectra in solution and in the solid state).

Addition of one electron to $[FeL_4H_{12}]^{-}$ and $[Fe_3L_8H_{22}]^{-}$ leads to doubly-negative charged systems. Spin density remains mainly localized on iron and coordinated oxygens, as observable from data collected in tables 1 and 2. In particular, the variation of spin density on the metal centers on comparing the two $[Fe_3L_8H_{22}]^{n-}$ systems ($n = 1$ and 2) is negligible, around 0.08 a.u. average value for this difference on considering the Mulliken and Natural analyses and around 0.11 a.u. using the Hirshfeld population analysis. The addition of one electron to $[Fe_3L_8H_{22}]^{-}$ leads instead to a reduction of spin density mainly for the sum of the atoms constituting the ligands. The fact that one-electron reduction has small influence on the electronic configuration of iron ions is confirmed by comparison of the iron atomic charges between $[Fe_3L_8H_{22}]^{-}$ and $[Fe_3L_8H_{22}]^{2-}$. In the first case, average values of 0.605 a.u. (Mulliken) and 1.255 (Natural) have been computed (M06/C-PCM calculations) and quite similar average charge have been obtained for the reduced compound, 0.533 a.u. (Mulliken) and 1.181 (Natural). The behavior towards reduction of $[Fe_3L_8H_{22}]^{-}$, in particular the apparently slight role of the metal centers, can be explained by study of the molecular orbitals of this compound. In particular, the lowest energy unoccupied orbitals are mainly localized on the π-systems of coordinated ligands and not on the metal centers (see figure 8).

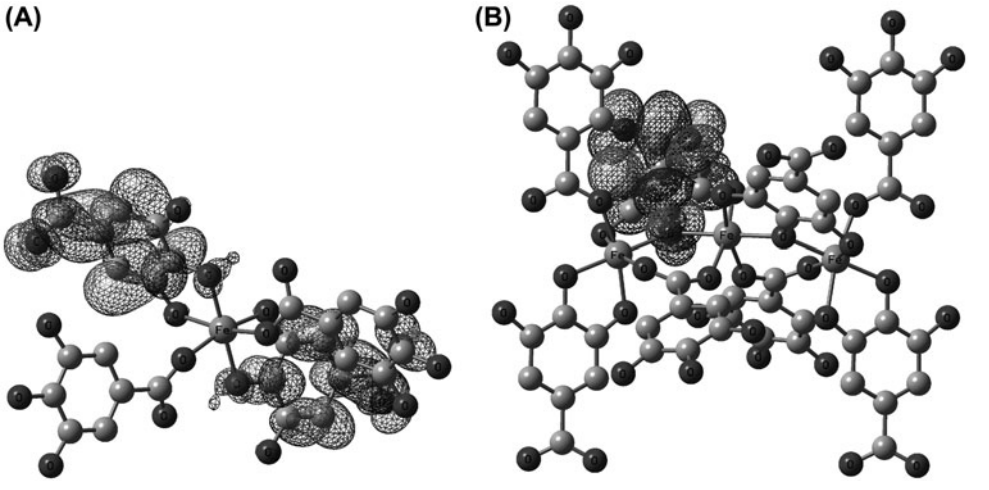

Figure 8. Plot of the LUMOs of $[FeL_4H_{12}]^-$ (A) and $[Fe_3L_8H_{22}]^-$ (B).

The computed data for the $[FeL_4H_{12}]^{n-}$ systems allow considerations comparable with those described for the tri-nuclear models. For both the oxidized and reduced models, the spin densities on iron are near the ideal value for free high-spin Fe(II). Moreover, the one-electron reduction leads to a decrease of spin density over the coordinated ligands also for the simpler model $[FeL_4H_{12}]^-$. In fact, as for $[Fe_3L_8H_{22}]^-$, also for $[FeL_4H_{12}]^-$ the low-energy unoccupied orbitals are localized on the conjugate bases of gallic acid (see figure 8).

Energies ($E+\Delta G_{solv}$) of the mono- and tri-nuclear complexes in oxidized and reduced forms have been used to study the relative oxidizing potentials of these models for iron gall inks [21]. Data are collected in table 3, together with those obtained at the same computational level for $[Fe(H_2O)_6]^{n+}$ ($n=2$, sextet state; $n=3$, quintet state) and $[Fe(EDTA)]^{n-}$ ($n=1$, sextet state; $n=2$, quintet state), used as references.

The energy difference calculable from the data presented in table 3 for the $[Fe(H_2O)_6]^{n+}$ couple is -0.22553 a.u. and corresponds to an experimental reduction potential (*vs*. NHE) of 0.77 V [22]. The energy variation from the oxidized to the reduced form of the iron-EDTA complex, -0.13092 a.u., is instead related to an experimental potential value of -0.12 V [22]. Assuming a linear relationship between experimental and computed data, we can estimate the reduction potentials of $[FeL_4H_{12}]^-$ and $[Fe_3L_8H_{22}]^-$. Both the models proposed in this work for iron gall inks have quite negative potentials for the one-electron reduction, about -0.27 V for the mononuclear system and -0.34 V for the trinuclear complex. The most negative potential is for the most complex system, i.e. the most similar to the experimental structure. In fact, the reduction of $[FeL_4H_{12}]^-$ is about 5 kcal mol^{-1}

Table 3. Energy values ($E+\Delta G_{solv}$, M06/C-PCM, a.u.) for systems $[FeL_4H_{12}]^{n-}$, $[Fe_3L_8H_{22}]^{n-}$ ($n=1$, 2), $[Fe(H_2O)_6]^{n+}$ ($n=2$, 3) and $[Fe(EDTA)]^{n-}$ ($n=1$, 2).

Model	Oxidized form	Reduced form
$[FeL_4H_{12}]^{n-}$	−2706.02468	−2706.14008
$[Fe_3L_8H_{22}]^{n-}$	−5534.66343	−5534.77144
$[Fe(H_2O)_6]^{n+}$	−581.90970	−582.13523
$Fe(EDTA)^{n-}$	−1223.16037	−1223.29129

more favored than that of $[Fe_3L_8H_{22}]^-$. However, in both cases the estimated potentials indicate a quite scarce oxidizing behavior of the iron complexes with gallic acid.

4. Conclusions

The results reported in this work on simple mono- and tri-nuclear models for iron gall inks strongly support the idea that a qualitatively correct description of the electronic structures of these compounds could be based on the presence of high-spin Fe(II) metal ions coordinated to partially oxidized conjugate bases of gallic acid, in agreement with previous studies on 3D periodic models. The partially radical character of the oxygen-donor polydentate ligands in these complexes can also explain the absorption properties of these materials.

The computed energy variations associated to one-electron reductions and their comparison with data obtained for other known iron complexes indicate that the oxidizing potential of iron gall inks is low. This evidence suggests that the direct oxidation of substrates of interest in the field of cultural heritage by iron gall inks is an improbable pathway for the commonly observed corrosion reactions.

Supplementary material

Examples of experimental absorption spectra of an iron gall ink in water solution and in the solid state. Experimental and computed IR spectra of gallic acid. Cartesian coordinates of the model compounds considered in this work.

Acknowledgements

Authors thank Ca' Foscari University for financial support. We acknowledge the CINECA Awards N. HP103I3CHF (2010) and N. HP10CRPVUO (2011) for the availability of high performance computing resources. Prof. Valerio Bertolasi, University of Ferrara, is gratefully acknowledged for support.

References

[1] (a) M. Zerdoun Bat-Yehouda. *Les encres noires au Moyen Age (jusqu'à 1600)* [Black Inks in the Middle Ages (until 1600)], Éditions du Centre National de la Recherche Scientifique, Paris (1983); (b) M. Budnar, M. Uršič, J. Simčič, P. Pelicon, J. Kolar, V.S. Šelih, M. Strlič. *Nucl. Instrum. Methods B*, **243**, 407 (2006); (c) M. Budnar, J. Simčič, Z. Rupnik, M. Uršič, P. Pelicon, J. Kolar, M. Strlič. *Nucl. Instrum. Methods B*, **219/220**, 41 (2004); (d) J.G. Neevel. In *The Iron Gall Ink Meeting Postprints*, J.E. Brown (Ed.), p. 33, University of Northumbria, Newcastle upon Tyne (2000); (e) V. Daniels. In *The Iron Gall Ink Meeting Postprints*, J.E. Brown (Ed.), p. 31, University of Northumbria, Newcastle upon Tyne (2000); (f) C.-H. Wunderlich. *Restauro*, **100**, 412 (1994); (g) C. Krekel, In *Tintenfrassschäden und ihre Behandlung* [Ink corrosion damage and its treatment], G. Banik, H. Weber (Eds.), W. Kohlhammer GmbH, Stuttgart (1999).

[2] C.-H. Wunderlich, R. Weber, G. Bergerhoff. *Z. Anorg. Allg. Chem*., **598/599**, 371 (1991).

[3] (a) V. Jančovičová, M. Ćeppan, B. Havlínová, M. Reháková, Z. Jakubíková. *Chem. Pap*., **61**, 391 (2007); (b) B. Wagner, E. Bulska. *Anal. Bioanal. Chem*., **375**, 1148 (2003); (c) V. Rouchon, M. Duranton, C. Burgaud, E. Pellizzi, B. Lavédrine, K. Janssens, W. de Nolf, G. Nuyts, F. Vanmeert, K. Hellemans. *Anal. Chem*., **83**, 2589 (2011); (d) S. Jurinovich, I. Degano, B. Mennucci. In *Proceedings of the First National Congress of the Division of Theoretical and Computational Chemistry of the Italian Chemical Society*, Pisa, p. 85 (2012); (e) J. Kolar, A. Štolfa, M. Strlič, M. Pompe, B. Pihlar, M. Budnar, J. Simčič, B. Reissland. *Anal. Chim. Acta*, **555**, 167 (2006); (f) J.G. Neevel. *Restaurator*, **16**, 143 (1995); (g) V. Rouchon Quillet, C. Remazeilles, T.P. Nguyen, J. Bleton, A. Tchapla. In *Durability of Paper and Writing*, J. Kolar, M. Strlič, J.B.

G.A. Havermans (Eds.), **56** (2004), National and University Library, Ljubljana (2004); (h) *Iron Gall Inks: On Manufacture, Characterisation, Degradation, And Stabilisation*, J. Kolar, M. Strlic (Eds.), National and University Library, Ljubljana (2006); (i) G. Banik, F. Mairinger, H. Stachelberger. *Restaurator*, **1/2**, 71 (1981); (j) M. Hey. *Restaurator*, **1/2**, 24–44 (1981); (k) O. Hahn. *Restauro*, **4**, 275 (1999).

[4] (a) G. Albertin, A. Albinati, S. Antoniutti, M. Bortoluzzi, S. Rizzato. *J. Organomet. Chem*., **702**, 45 (2012); (b) M. Bortoluzzi, G. Paolucci, B. Pitteri. *Polyhedron*, **30**, 1524 (2011); (c) M. Bortoluzzi, E. Bordignon, G. Paolucci, B. Pitteri. *Polyhedron*, **26**, 4936 (2007); (d) E. Bordignon, M. Bortoluzzi. *Inorg. Chem. Commun*., **8**, 763 (2005).

[5] T.A. Halgren. *J. Comput. Chem.*, **17**, 490 (1996).

[6] (a) H.J. Monkhorst, J.D. Pack. *Phys. Rev. B*, **13**, 5188 (1976); (b) H.J. Monkhorst, J.D. Pack. *Phys. Rev. B*, **16**, 1748 (1977).

[7] J.P. Perdew, K. Burke, M. Ernzerhof. *Phys. Rev. Lett.*, **77**, 3865 (1996).

[8] (a) A.D. Becke. *J. Chem. Phys*., **98**, 5648 (1993); (b) A.D. Becke. *Phys. Rev. A*, **38**, 3098 (1988); (c) P. Geerlings, F. De Proft, W. Langenaker. *Chem. Rev.*, **103**, 1793 (2003); (d) T. Ziegler. *Chem. Rev.*, **91**, 651 (1991).

[9] Y. Zhao, D.G. Truhlar. *Theor. Chem. Acc.*, **120**, 215 (2008).

[10] (a) T.H. Dunning, P.J. Hay. In *Modern Theoretical Chemistry*, H.F. Schafter (Ed.), Vol. 3, pp. 1–28, Plenum Press, New York (1976); (b) T.H. Dunning. *J. Chem. Phys*., **55**, 716 (1971).

[11] (a) A. Bergner, M. Dolg, W. Kuechle, H. Stoll, H. Preuss. *Mol. Phys*., **80**, 1431 (1993); (b) P. Schwerdtfeger, M. Dolg, W.H.E. Schwarz, G.A. Bowmaker, P.D.W. Boyd. *J. Chem. Phys*., **91**, 1762 (1989).

[12] A.D. McLean, G.S. Chandler. *J. Chem. Phys.*, **72**, 5639 (1980).

[13] (a) P.J. Hay, W.R. Wadt. *J. Chem. Phys*., **82**, 299 (1985); (b) L.E. Roy, P.J. Hay, R.L. Martin. *J. Chem. Theory Comput*., **4**, 1029 (2008).

[14] (a) V. Barone, M. Cossi. *J. Phys. Chem. A*, **102**, 1995 (1998); (b) M. Cossi, N. Rega, G. Scalmani, V. Barone. *J. Comput. Chem*., 669 (2003).

[15] C.J. Cramer. *Essentials of Computational Chemistry*, 2nd Edn, John Wiley and Sons, Chichester (2004).

[16] (a) R.S. Mulliken. *J. Chem. Phys*., **23**, 1833 (1955). (b) A.E. Reed, L.A. Curtiss, F. Weinhold. *Chem. Rev.*, **88**, 899 (1988). (c) F.L. Hirshfeld. *Theor. Chim. Acta*, **44**, 129 (1977).

[17] M.J. Frisch, G.W. Trucks, H.B. Schlegel, G.E. Scuseria, M.A. Robb, J.R. Cheeseman, G. Scalmani, V. Barone, B. Mennucci, G.A. Petersson, H. Nakatsuji, M. Caricato, X. Li, H.P. Hratchian, A.F. Izmaylov, J. Bloino, G. Zheng, J.L. Sonnenberg, M. Hada, M. Ehara, K. Toyota, R. Fukuda, J. Hasegawa, M. Ishida, T. Nakajima, Y. Honda, O. Kitao, H. Nakai, T. Vreven, J.A. Montgomery, Jr., J.E. Peralta, F. Ogliaro, M. Bearpark, J.J. Heyd, E. Brothers, K.N. Kudin, V.N. Staroverov, T. Keith, R. Kobayashi, J. Normand, K. Raghavachari, A. Rendell, J.C. Burant, S.S. Iyengar, J. Tomasi, M. Cossi, N. Rega, J.M. Millam, M. Klene, J.E. Knox, J.B. Cross, V. Bakken, C. Adamo, J. Jaramillo, R. Gomperts, R.E. Stratmann, O. Yazyev, A.J. Austin, R. Cammi, C. Pomelli, J.W. Ochterski, R.L. Martin, K. Morokuma, V.G. Zakrzewski, G.A. Voth, P. Salvador, J.J. Dannenberg, S. Dapprich, A.D. Daniels, O. Farkas, J.B. Foresman, J.V. Ortiz, J. Cioslowski, D.J. Fox. *Gaussian 09, Revision B.01*, Gaussian, Inc., Wallingford, CT (2010).

[18] (a) *Spartan 08,* (*Version 1.1.1*), Wavefunction, Inc., Irvine, CA (2009); (b) W.J. Hehre, *A Guide to Molecular Mechanics and Quantum Chemical Calculations*, Wavefunction, Inc., Irvine, CA (2003).

[19] S. Zaccaron, R. Ganzerla, M. Bortoluzzi. *Scienze a Ca' Foscari*, **2** (2013).

[20] (a) H. Kipton, J. Powel, M.C. Taylor. *Aust. J. Chem*., **35**, 739 (1982); (b) M.C. Carter. *J. Mol. Struct*., **831**, 26 (2007).

[21] M. Cossi, M.F. Iozzi, A.G. Marrani, T. Lavecchia, P. Galloni, R. Zanoni, F. Decker. *J. Phys. Chem. B*, **110**, 22961 (2006).

[22] N.N. Greenwood, A. Earnshaw. *Chemistry of the Elements*, Pergamon Press, Oxford (1984).